The Visual Hull of Smooth Curved Objects

Andrea Bottino and Aldo Laurentini, *member, IEEE*

Dipartimento di Automatica ed Informatica, Politecnico di Torino,

Corso Duca degli Abruzzi 24, 10129 Torino, Italy

Corresponding author: aldo.laurentini@polito.it

Abstract. The visual hull is a geometric entity that relates the shape of a 3D object to its silhouettes or shadows. This paper develops the theory of the visual hull of generic smooth objects. This is performed by relating the surface of the visual hull of the object to its aspect graph. We show that the visual hull can be constructed using patches of the surfaces that partition the viewpoint space of the aspect graph. In particular, the visual events *tangent crossing* and *triple point* generate the relevant surfaces. A further analysis, based on the shape of the surface of the object at the tangency points of these surfaces, allows selecting their active parts, i.e. the surface patches which could actually bound the visual hull. Finally, an algorithm for computing the visual hull starting from the active patches is outlined.

Index Terms. Computer vision, aspect, aspect graphs, silhouettes, visual hull, smooth curved objects

1. INTRODUCTION

Many algorithms for reconstructing or recognizing 3-D objects from 2-D image features are based on particular lines called *image contours*. This approach mimics to some extent the human vision, since we are often able to understand the solid shape of an object from a few image lines laid out on a plane [13], [16].

The lines called *occluding contours* (*apparent contours*, *limbs*) are the projection onto the image plane of the *contour generators* of the objects. A contour generator is a locus of points of the object surface where there is a depth discontinuity along the line of sight. Ponce and Kriegman [18] and Forsyth [12] have investigated the relation between the occluding contours and the surface of smooth objects.

If we restrict ourselves to the contours occluding the background, usually easier to determine, we obtain silhouette-based recognition and reconstruction techniques. For instance, *Volume Intersection* reconstructs 3D shapes from multiple silhouettes [1], [6], [35]. The introduction of the geometric concept of *visual hull* [20] puts recognizing and reconstructing 3D shapes from silhouettes on a firm theoretical ground. The contours occluding the background are also at the basis of many techniques for extracting shape and orientation of rotating objects (see for instance the recent paper [24]).

If we consider the contours that occlude both the background and the object itself, together with the image lines called *edges,* projections of the *creases* of the object (surface normal discontinuities), we obtain line drawings that can be organized into the *aspect graph*, a user-centered representation first proposed for object identification in 1979 by Koenderink and van Doorn [17].

Visual hull and aspect graph of an object are linked together since they based, entirely or in part, on its occluding contours. A new global visibility structure, the *visibility complex*, introduced in 2D by Pocchiola and Vegter [30], and extended in 3D by Durand et al. [8][9], appears promising for dealing both with aspect graph and visual hull. Petitjean used this data structure for efficiently computing the visual hull of polygons and polyhedra [27].

This paper exploits the link between visual hull and aspect graph for developing the theory of the visual hull of concave objects bounded by smooth curved surfaces. In particular, we have found that the surface of the visual hull that bounds the concavities of the object consists of sub-patches of two ruled surfaces used for partitioning the view space of the aspect graph. These surfaces are

related to two particular *visual events* (changes of topology of the aspects) of the aspect graph, called *tangent crossing* and *triple points*.

In the rest of the Introduction we overview the basic concepts of visual hull and aspect graph, and present a summary of the paper.

1.1 The Visual Hull

The visual hull is a geometric entity that allows understanding capabilities and limits of the techniques for comparing or understanding the shape of 3D objects using their silhouettes or shadows [19]. Broadly speaking, the visual hull **VH(O,VR)** of an object **O** relative to a viewing region **VR** of R^3 is the largest object that produces the same silhouettes (or shadows) as **O** observed from viewpoints (lighted from point lights) belonging to **VR**. The visual hull is also the closest approximation of **O** that can be obtained by volume intersection from silhouettes (or shadows) obtained with viewpoints (or point light sources) belonging to **VR**.

All the visual hulls relative to viewing regions which: 1) completely enclose **O**; 2) do not share any point with the convex hull of **O**; are equal. This is the external visual hull of **O**, or simply the visual hull **VH(O)**. If the viewing region is bounded by the object **O** itself, we have the internal visual hull **IVH(O)**. The external visual hull is relevant to most practical situations.

Visual hull, internal visual hull and convex hull **CH(O)** are related by the following inequalities: **IVH(O)**≤ **VH(O)** ≤ **CH(O)**. For convex objects, all these entities are coincident.

The visual hull allows answering questions such as: can the shape of an object be fully determined from its silhouettes? If not, which is the closest approximation that can be obtained? Can two objects be distinguished from their silhouettes? The answers to the previous questions are: an object can be reconstructed from its silhouettes iff it is coincident with its visual hull; the closest approximation that can be obtained is the visual hull; we can tell an object from another using silhouettes iff their visual hulls are different.

An intuitive physical construction of the visual hull of is as follows. Suppose filling the concavities of the object with soft material. The visual hull can be obtained by scraping off the excess material with a ruler grazing the hard surface of the object in all possible ways. In Fig.1, **O** is one half of an object of revolution. **CH(O)** is its convex hull, where the concavity has been filled. The last image shows the visual hull **VH(O)**, and I particular S"$_{VH}$, the surface of the visual hull that covers the concavity, produced by the ruler.
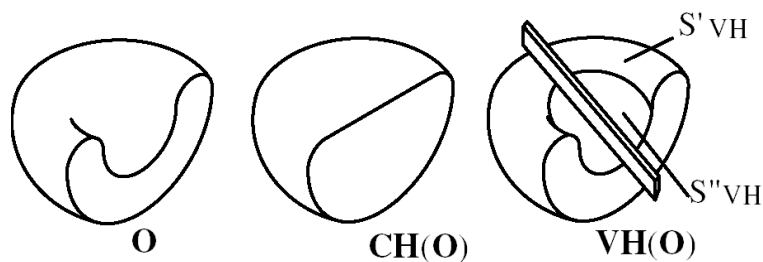

Fig.1. An object **O**, its convex hull **CH(O)** and its visual hull VH(O)

Algorithms for computing the visual hulls of polygons, polyhedra and solids of revolution can be found in [19], [20] and [27], to which the reader is referred for further details. Developments and applications of the visual hull idea can be found in [21], [22] and [23].

1.2 The Aspect Graph

The basic idea of the *aspect graph* is clustering the infinite views of an object into a finite set of representative views. The views to be clustered are the line drawings consisting of the occluding contours and edges of the object image. For most viewpoints these views are topologically stable, since perturbing the viewpoint in a small ball does not change their topological structure. The range of all possible viewpoints can be partitioned into a set of maximal open regions where the structure of the line drawing, also called *aspect*, is stable. Crossing the boundaries between these regions produces a topological change in the aspects known as *visual event*. Aspects and visual events are arranged into a graph structure, the *aspect graph* (AG), where each node is labeled with an aspect and each arc represents a visual event. For perspective AG, each aspect corresponds to a connected open volume of viewpoints, and each visual event to a boundary surface. For the parallel AG,

aspects and visual events correspond to open connected areas and boundary lines on the Gaussian sphere. The parallel aspect graph is a sub-graph of the perspective aspect graph, since not any perspective aspect is also a parallel aspect.

Constructing the AG requires determining the catalogue of the possible visual events and the related boundary surfaces, which is relatively easy for planar faces object (see [14]). Several authors have studied the more complex visual events of curved surfaces. A possible approach is using the *singularity theory* for determining the visual events as the singularities of the *visual mapping,* which maps the surface of the object onto the image plane [16], [15], [31], [32], [26], [5]. Other approaches have also been used [11], [34]. For a comparison of the catalogues presented, the reader is referred to [11]. Anyway, in this paper we will be only concerned with two simple and universally recognized visual events.

Algorithms for constructing the aspect graphs have been given for polyhedra, articulated objects, solids of revolution and various categories of curved objects under parallel and perspective projection. For further details the reader is referred to the survey paper [3], to [4], [10], [11], [28], [29] and [33], and to the comprehensive bibliography reported in these papers.

1.3 SUMMARY OF THE PAPER

The rest of this paper is organized as follows.

1) In Section 2 we determine a necessary condition for a point to belong to the part of surface of the visual hull which bounds the concavities of the object. This condition links together visual hull and aspect graph. It states that the point must lay on either of two particular ruled surfaces that partition the viewing space for constructing the aspect graph. Algorithms for computing these surfaces can be found in the literature on aspect graphs [28].

2) In Section 3 we determine more strict necessary conditions. This is obtained by performing a detailed analysis, based on the geometry of the curved object at the tangency

points of these surfaces. This analysis allows discarding entirely several of these surfaces or in any cases some of their parts. The patches that survive this elimination process are called *locally active*.

3) In Section 4 we sketch an algorithm for computing the visual hull, based on the locally active patches.

2 A NECESSARY CONDITION FOR A POINT TO BELONG TO THE SURFACE OF THE VISUAL HULL

Let us consider an object **O** bounded by a *generic* smooth surface. Obviously, the line drawings of smooth objects only include occluding contours. The adjective "generic" refers to a surface without exceptional zero probability alignments. This extends to curved surfaces the 2D idea of generic polygon (three vertices do not lie on the same straight line) and the 3D idea of generic polyhedron (two edges not belonging to the same face do not lie on the same plane, and four edges do not lie on the same ruled quadric surface). In particular, generic for a smooth surface means that there can exist only *isolated* lines (they do not form surfaces) tangent at more than three points. For a more formal definition, the reader is referred to [7]. Aspect graphs and visual events of generic smooth surfaces have been considered explicitly in several papers, as [5], [28], and implicitly in many other papers on the subject.

In general, the surface S_{VH} of **VH(O)** can be divided into two parts: S'_{VH} coincident with the surface S of **O**, and S''_{VH}, which "covers" some concavities of **O** (see Fig.1 for an example). Actually, S''_{VH} could also bound volumes not connected to **O** (see [19]). In this section we will relate S''_{VH} to the boundary surfaces of the viewing space corresponding to two particular visual events.

For the following developments, it is important to recall that a visual *line* relative to an object **O** is a straight line not sharing any point with **O**. A formal definition of visual hull is as follows [9].

Prop.1-A point **p** *belongs to* **VH(O)** *iff no visual line relative to* **O** *passes through* **p**.

In the following we will use many times this condition for showing that a point does not belong to the visual hull. From Prop.1 it follows that:

Prop.2- If a point **p** *belongs to* S_{VH}, *there are visual lines relative to* **O** *arbitrarily close to* **p**.

From these statements we can derive a further necessary condition for a point to belong to S_{VH}.

Prop. 3- If a point **p** *belongs to* S_{VH}, *through* **p** *passes at least one straight line intersecting* **O** *only in boundary points.*

Proof. By contradiction, let us assume that through **p**∈ S_{VH} no such line passes. It follows that any line through **p** belongs to either of two categories: 1) lines not intersecting **O**; 2) lines sharing with **O** also interior points. If there are lines of the first category, that is visual lines, **p** does not belong to **VH(O)** because of *Prop.1*. If all the lines passing through **p** belong to the second category, **p** cannot belong to S_{VH} since the condition of *Prop.2* cannot be met. In this case in fact, there are no visual lines arbitrarily close to **p**, since each possible visual line L' passing at an infinitesimal distance from **p** lies at an infinitesimal distance from a line L through **p**, and therefore also intersects **O** in interior points (see Fig. (2)). Thus the hypothesis is contradicted and the proposition proved.
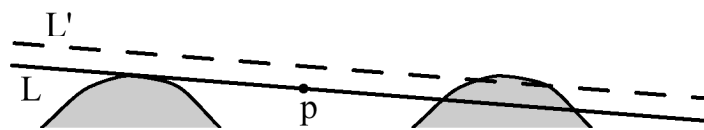

Fig.2. **p** cannot belong to S_{VH} if all lines through **p** are as L.

From the previous discussion it follows that, for finding points of S_{VH}, we can restrict ourselves to consider only points of straight lines tangent to the surface S of the object.

In the rest of this section we will consider the cases of lines making one, two or three contacts with S. It has been already observed that a generic surface also admits lines tangent at more than 3 points, but these lines are isolated and do not form surfaces.

It is clear that a line L making contact at only one point **p** with S cannot form boundary surfaces of the visual hull. Only **p** belongs to S_{VH}, since through any other point **p'** of L pass visual lines obtained with an infinitesimal rotation $\partial\alpha$ of L about **p'**, as L' in Fig 3. Since by hypothesis L does not intersect S elsewhere, this is true also after an infinitesimal rotation of the line.

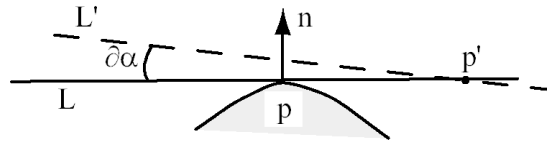Fig.3. Only **p** belongs to S_{VH}. Through any other point **p'** pass visual lines as L'.

In the following sub-sections we will discuss in detail the cases of lines making two or three contacts with **O**.

2.1. The Case of Bi-tangent Lines

Straight lines tangent at two different points of S do not yield surfaces but fill volumes, so we need a radical pruning of these lines. For understanding if a bi-tangent line can contain points of the surface S''_{VH} of the visual hull, we will consider the *normals* to S at the tangency points, and investigate whether they are compatible or not with visual lines passing through points of the tangent line.

Let us consider a line L tangent at two points $\mathbf{p}_1$ and $\mathbf{p}_2$ of S. Assume the surface normals at $\mathbf{p}_1$ and $\mathbf{p}_2$ be $\mathbf{n}_1$ and $\mathbf{n}_2$, and project orthographically these entities along L, together with infinitesimal segments of the contour generators containing $\mathbf{p}_1$ and $\mathbf{p}_2$. Also let P be a plane containing L and the unit vector $\mathbf{n} = (\mathbf{n}_1 + \mathbf{n}_2)/|\mathbf{n}_1 + \mathbf{n}_2|$ (see Fig. 4 (a)).
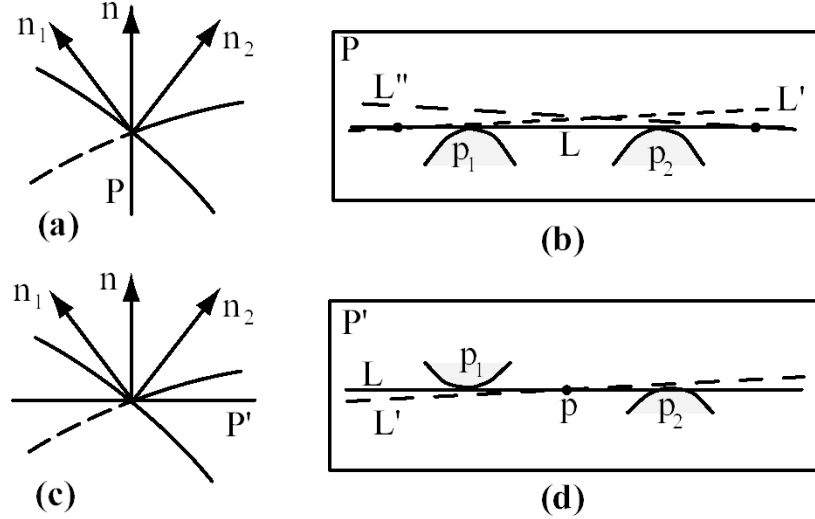
Fig.4- For $\mathbf{n}_1\mathbf{x}\mathbf{n}_2 \neq 0$, no point of L, excluding $\mathbf{p}_1$ and $\mathbf{p}_2$, belongs to S_{VH}

The points $\mathbf{p}_1$ and $\mathbf{p}_2$ divide L into two exterior half-open infinite segments and one open interior segment. Let us consider the intersection of P and $\mathbf{O}$ (Fig. 4(b)). It is clear that the exterior segments cannot contain points belonging to S''_{VH}, since in P there are visual line as L' and L", obtained with infinitesimal rotations of L, passing through any point of both segments.

Let us consider the interior segment. In P there are visual lines passing above the segment at an arbitrarily small distance, but no visual lines passes through points of the segment.

The situation is different in a plane as P' in Fig.4(c), normal to P. Its intersection with S is shown in Fig. 4(d). It is clear that through any point $\mathbf{p}$ of the interior segment passes a visual line as L' compatible with the local geometry.

Since the previous statements hold for all cases where the vector product $\mathbf{n}_1\mathbf{x}\mathbf{n}_2$ is different from zero, we have:

Prop. 4: a necessary condition for a bi-tangent line to contain points of S''_{VH} is that $\mathbf{n}_1\mathbf{x}\mathbf{n}_2=0$, that is $\mathbf{n}_1=\mathbf{n}_2$ or $\mathbf{n}_1=-\mathbf{n}_2$.

This result links together visual hull and aspect graphs, since lines satisfying this condition produce the multi-local visual event known as *tangent crossing* [5], [11], [15], [28]. The visual event occurs when two limbs meet at a point and share a common tangent, forming a tacnode (Fig (5)).
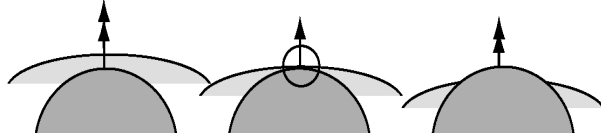
Fig. 5. Tangent crossing

For parametric surfaces $\mathbf{p}=\mathbf{p}(u,v)$, the equations that determine the tangency points for these lines are:

$$[\mathbf{p}_1(u_1,v_1) - \mathbf{p}_2(u_2,v_2)] \bullet \mathbf{n}_1(u_1,v_1)=0$$

$$[\mathbf{p}_1(u_1,v_1) - \mathbf{p}_2(u_2,v_2)] \bullet \mathbf{n}_2(u_2,v_2)=0 \qquad\qquad (1)$$

$$[[\mathbf{p}_1(u_1,v_1) - \mathbf{p}_2(u_2,v_2)] \times \mathbf{n}_1(u_1,v_1)]\bullet \mathbf{n}_2(u_2,v_2)=0$$

Where $\bullet$ indicates the dot product, and the surface normals are the vector product of the partial derivatives: $\mathbf{n}(u,v)=\mathbf{p}_u(u,v)\times \mathbf{p}_v(u,v)$. These are 3 equations in the four variables $u_1,$ $v_1,$ $u_2,$ $v_2,$ and thus determine the curves described by $\mathbf{p}_1$ and $\mathbf{p}_2$ on the surface S. Similar equations can be written for implicit surfaces (see [28]). A line joining points $\mathbf{p}_1$ and $\mathbf{p}_2$ generates a ruled boundary surface of the viewing space of the aspect graph that can also be a boundary of the visual hull.

Observe that not all the surfaces determined by equations (1) are relevant to our purposes, since we must select the surfaces, or their parts, where the generating tangent line does not intersect **O** elsewhere. In other words, we are only interested in visual events that happen on the boundary of the silhouette of the object.

2.2 The Case of Tri-tangent Lines

In this case the relationship with the aspect graph boundary surfaces is immediately established, since tri-tangent lines produce the visual event known as *triple point* [5], [11], [15], [28] (see Fig. 6).
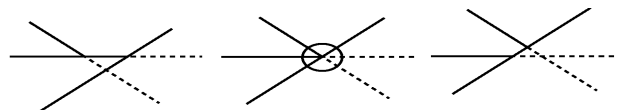

Fig. 6. Triple point

Also in this case it is easy to write the equations that determine the three tangency points $\mathbf{p}_1$, $\mathbf{p}_2$ and $\mathbf{p}_3$. For parametric surfaces:

$$[\mathbf{p}_1(u_1,v_1) - \mathbf{p}_2(u_2,v_2)\,] \bullet \mathbf{n}_3(u_3,v_3)=0$$

$$[\mathbf{p}_2(u_2,v_2) - \mathbf{p}_3(u_3,v_3)\,] \bullet \mathbf{n}_2(u_2,v_2)=0 \qquad\qquad (2)$$

$$[\mathbf{p}_3(u_3,v_3) - \mathbf{p}_1(u_1,v_1)\,] \bullet \mathbf{n}_1(u_1,v_1)=0$$

$$[\mathbf{p}_1(u_1,v_1) - \mathbf{p}_2(u_2,v_2)\,]\mathrm{x}[\mathbf{p}_1(u_1,v_1) - \mathbf{p}_3(u_3,v_3)\,]=0$$

The first three equations state the tangency conditions at $\mathbf{p}_1$, $\mathbf{p}_2$ and $\mathbf{p}_3$. The last equation states that the three points are collinear. The equations for the implicit case can be found in [28]. Since a 3D direction has two degrees of freedom, in the last vector equation only two scalar components are independent. This makes five equations in the six variables $u_1,\ v_1,\ u_2,\ v_2,\ u_3,\ v_3$, which describe three curves on the surface S. The lines passing through any two of the three points describe the ruled surface which could bound the visual hull.

As for the surfaces produced by be-tangent lines, the relevant surfaces generated by equations (2) are those where the generating three-tangent line does not intersect **O** elsewhere.

3. THE LOCALLY ACTIVE SURFACES

Let us summarize the results of the previous section:

*Prop.5 - A necessary condition for a point to belong to S"$_{VH}$ is that it lies on the boundary ruled surfaces of the aspect graph corresponding either to the visual event tangent crossing or to the visual event triple point. The relevant parts of these surfaces are those where the generating tangent lines shares with **O** the tangency points only.*

Before building the visual hull using these surfaces, we will submit the surfaces to an elimination process that will discard several of them, and in any case some of their parts. This process will be based on a closest *local* analysis, which will consider not only the surface normals, but also the shape of the object at the tangency points. The patches that survive this elimination

process will be called *locally active*. This attribute will be applied also to the surfaces that contain these patches and to the segments of straight lines that generate the surfaces.

The two following subsections will be devoted to determine the locally active patches generated by bi-tangent and three-tangent lines

3.1 Locally Active Segments of Bi-tangent Lines

The technique that we will use for eliminating, completely or in part, tangent lines and the surface they form, consists in finding, if they exist, visual lines passing through points of the tangent line and compatible with the shape of the surface *near* the tangency point $\mathbf{p}_1$ and $\mathbf{p}_2$. For this purpose, we will attempt to perform an infinitesimal rotation of the tangent line L about one of its points without intersecting the infinitesimal surface patches near $\mathbf{p}_1$ and $\mathbf{p}_2$.

For dealing with the geometry of an infinitesimal patch of a smooth surface near a point $\mathbf{p}$ it will be helpful to consider its Gaussian curvature K($\mathbf{p}$), the product of the principal curvatures $k_1(\mathbf{p})$ and $k_2(\mathbf{p})$. Let us recall that near a point $\mathbf{p}$ the surface can be approximated by:

$$2z = k_1(\mathbf{p})x^2 + k_2(\mathbf{p})\,y^2$$

if the axis Z is normal to the surface at $\mathbf{p}$ and the axes X and Y are oriented along the principal directions. Approximating the surface surrounding a point with a quadric patch implies discarding higher order terms, which vanish faster than the quadratic terms approaching $\mathbf{p}$.
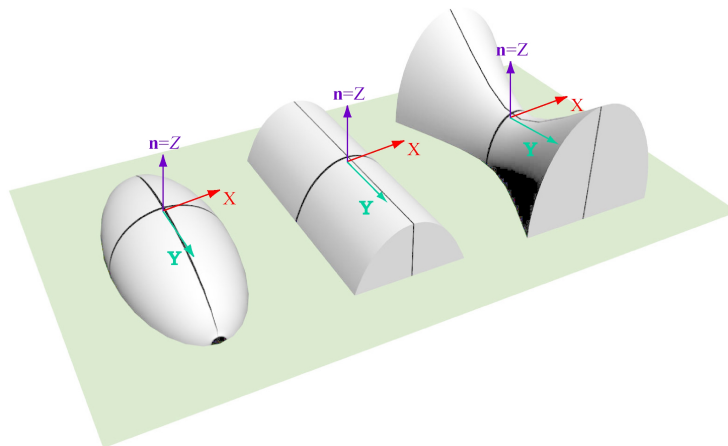

Fig. 7. Surface approximations

This surface turns out to be: 1) a paraboloid if $K(\mathbf{p})>0$, 2) a saddle-shaped hyperboloid if $K(\mathbf{p})<0$; 3) a cylinder if $K(\mathbf{p})=0$ and $k_1(\mathbf{p})=0$, or $k_2(\mathbf{p})=0$, but not both [25] (see Fig.7). We need not to consider planar points where $k_1(\mathbf{p}) = k_2(\mathbf{p})=0$, since generic surfaces can have only isolated planar points. On a generic surface, points whose Gaussian curvature is strictly positive (*elliptic points*), or strictly negative (*hyperbolic points*), forms open areas separated by curves whose points have zero Gaussian curvature (*parabolic points*)[1], [28].

Performing an infinitesimal rotation of L about one of its point compatible with the local geometry requires determining the limits imposed by this geometry. Let us consider the pencil of lines passing through a point $\mathbf{p}$ of L and tangent to S near $\mathbf{p}_1$ (or $\mathbf{p}_2$). In the Appendix we show that, both for elliptic and hyperbolic points, these lines touch S along the planar curve intersection of S and a plane passing through the Z axis of the local coordinate system. Near $\mathbf{p}_1$ (or $\mathbf{p}_2$) this curve is coincident with the contour generators C_1 (or C_2) produced by a pencil of lines of sight parallel to L, and can be approximated near $\mathbf{p}_1$ (or $\mathbf{p}_2$) **with** arbitrarily high precision by a circle with radius $1/k$, where k is the normal curvature. For a parabolic point, the lines passing through $\mathbf{p}$ touch S along the straight segment shared by the cylindrical approximation of the patch and the tangent plane.
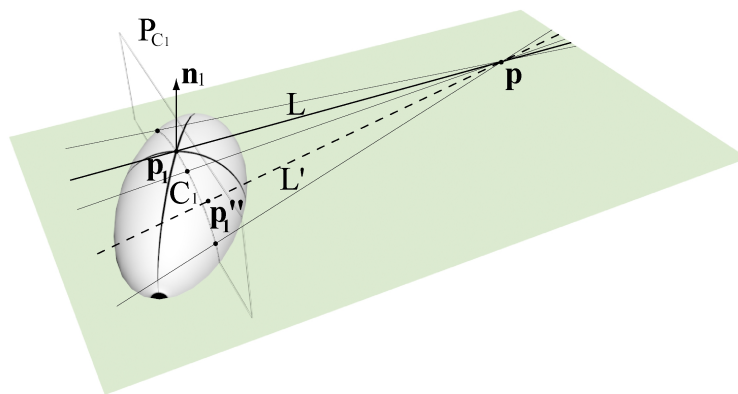

Fig. 8

Let $P_{C1 \text{ and }} P_{C2}$ be the planes normal to S at $\mathbf{p}_1$ and $\mathbf{p}_2$ and containing C_1 and C_2, and let **p1**" and $\mathbf{p}_2$" be the intersections of the rotated line L' with these planes. Now consider one of these

points, for instance $\mathbf{p}_1$"(Fig. 8). It is clear that L' does not intersect S near $\mathbf{p}_1$ if $\mathbf{p}_1$" lies in P_{C1} on the side of the contour generator marked by the external normal $\mathbf{n}_1$. Clearly, L' is a visual line iff it is possible to satisfy this condition at both the tangency points.

In the following we will consider separately the two cases **$\mathbf{n}_1$= $\mathbf{n}_2$ and $\mathbf{n}_1$= -$\mathbf{n}_2$**

3.1.1 Locally Active Segments for $\mathbf{n}_1$= $\mathbf{n}_2$

Observe first that only the interior segment of the tangent line could be locally active. This is easily seen considering the section of **O** made by the plane P_N containing $\mathbf{n}_1$ and $\mathbf{n}_2$. This section is as that shown in Fig.4(b), and the same argument applies. Thus, we must only investigate the interior segment.

The case $\mathbf{n}_1$= $\mathbf{n}_2$ generates six sub-cases, since each tangency point can be elliptic, parabolic or hyperbolic. We will consider the sub-cases in the following order: *elliptic-elliptic, parabolic - elliptic, parabolic-parabolic, hyperbolic-parabolic, hyperbolic-hyperbolic,* and *hyperbolic-elliptic.*

For each sub-case we show a figure containing:

- the tangent line L and, if it exists, the visual line L' obtained by a rotation of L about one of its points **p**;

- the tangency points $\mathbf{p}_1$ and $\mathbf{p}_2$ of L and the corresponding surface normals $\mathbf{n_1}$ and $\mathbf{n_2}$;

- two segments of paraboloid, hyperboloid, or cylinder according to the Gaussian curvature at $\mathbf{p}_1$ and $\mathbf{p}_2$ cut by planes parallel to P_T;

- the plane P_T tangent at $\mathbf{p}_1$ and $\mathbf{p}_2$;

- the planes P_{C1} and P_{C2} containing C_1 and C_2 near $\mathbf{p}_1$ and $\mathbf{p}_2$;

- the intersections $\mathbf{p}_1$" and $\mathbf{p}_2$" of L' and P_{C1} and P_{C2}.

For each case we will show a perspective view of these entities, and an orthographic projection along L onto a plane P. For simplicity, in the perspective view we omit P_T, and in P the entities projected will be indicated with the symbols of their 3D counterparts. The direction of the projectors is always from $\mathbf{p}_2$ to $\mathbf{p}_1$.

The sub-case elliptic-elliptic

Let us consider a point **p** of the interior segment (Fig. 9). Clearly an infinitesimal rotation δ_α of L about **p** in the tangent plane P_T generates a visual line L', since both $\mathbf{p}_1$" and $\mathbf{p}_2$" lie on the external side of C_1 and C_2, as shown by their projections onto the plane P. Therefore, the interior segment is not locally active.
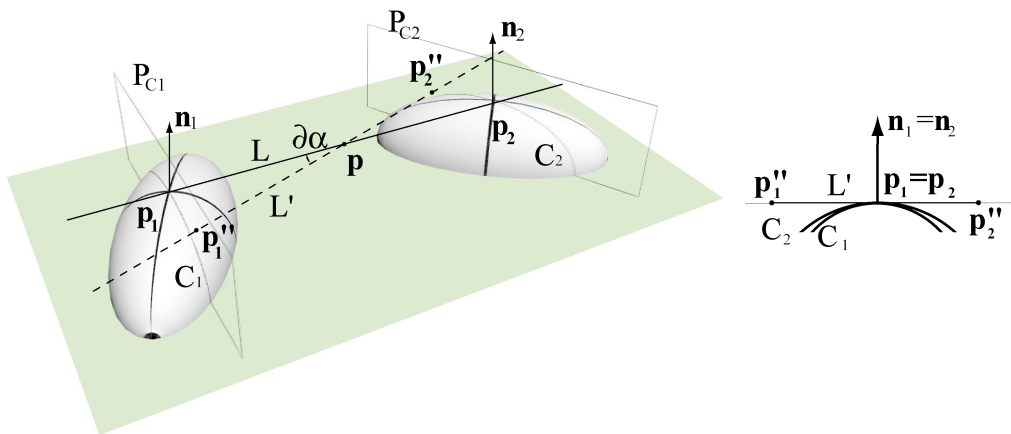

Fig. 9

The sub-case parabolic-elliptic

Also this case does not produce an active segment. A visual line through any point **p** of the interior segment can be obtained as follows (Fig.10). Perform first a rotation $\partial\alpha$ of L about **p** in the tangent plane P_T, then a rotation $\partial\beta$ in a plane normal to P_T. This produces the visual line L', and also in this case the segment is not locally active.
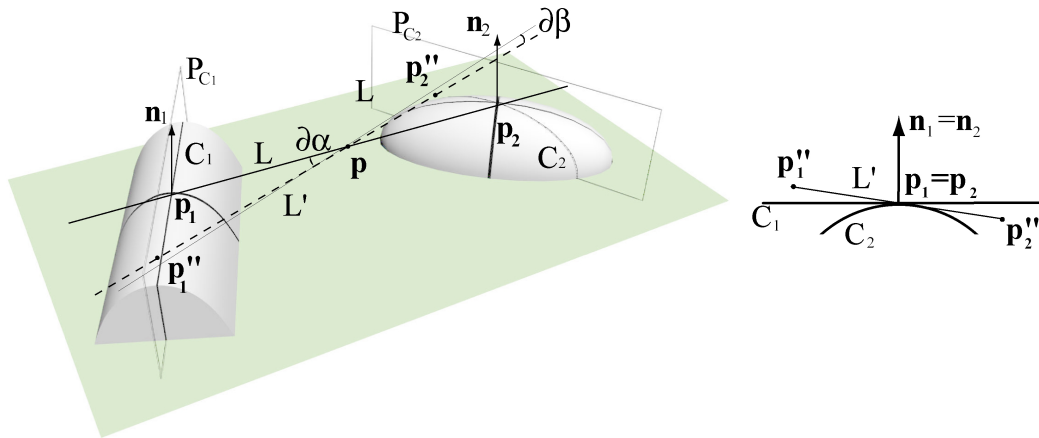
Fig. 10

The sub-case parabolic-parabolic

In this case the parallel projections along L of the contour generators are coincident. Understanding if a rotation of L compatible with the surface at the tangency points is possible (Fig.11) would require a more detailed model of the surface at the tangency points, involving higher order terms. However, this is not necessary, since for generic surfaces this is a limit situation and there are only isolated tangent lines of this kind [28].
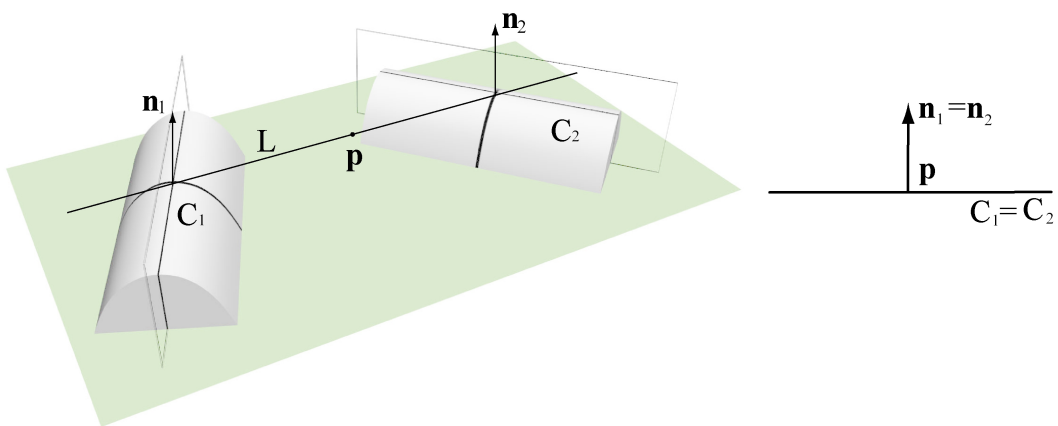

Fig. 11

The sub-case hyperbolic-parabolic

Inspecting Fig 12 shows that no rotation exists able to produce a visual line. In fact, for any rotated line L* such that p_1" lies above C_1, p_2" lies under the line C_2, as shown by the projection of these entities onto the plane P. Thus the internal segment is locally active.
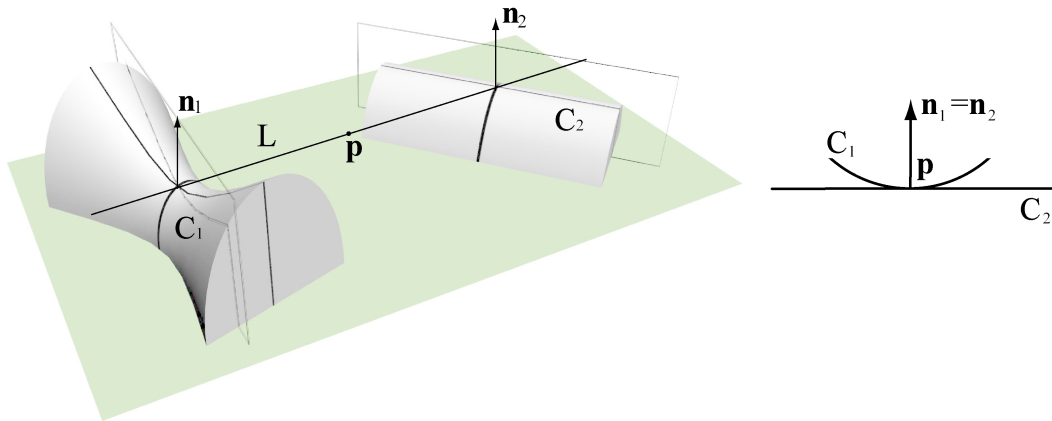

Fig. 12

The sub-case hyperbolic-hyperbolic

As before no visual line trough **p** can be obtained (Fig.13). Thus also in this case the internal segment is locally active.
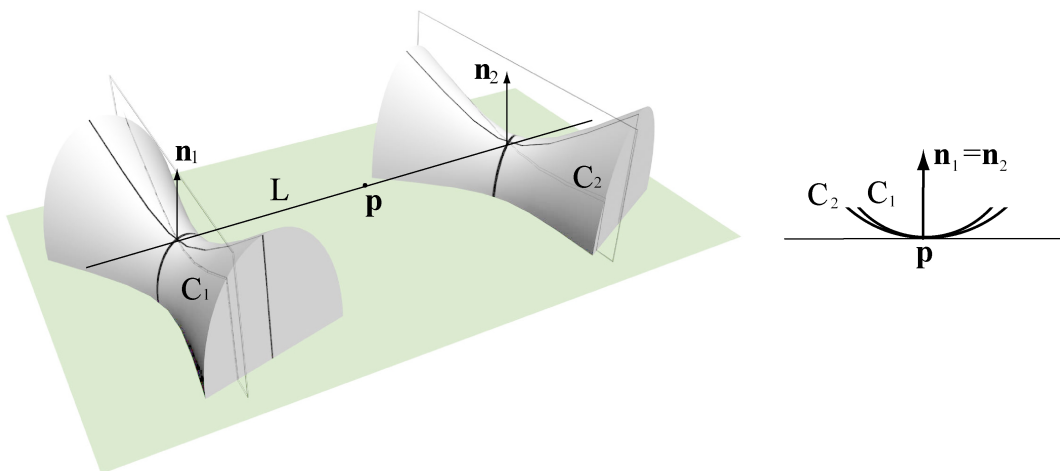

Fig. 13

The sub-case hyperbolic-elliptic

This sub-case (Fig.14) requires a more complex analysis, involving the values of the curvature of the contour generators at $\mathbf{p}_1$ and $\mathbf{p}_2$. These normal curvatures can be computed using Euler's formula:

$$k(\theta) = k_1(\mathbf{p})cos^2\theta + k_2(\mathbf{p})\ sin^2\theta$$

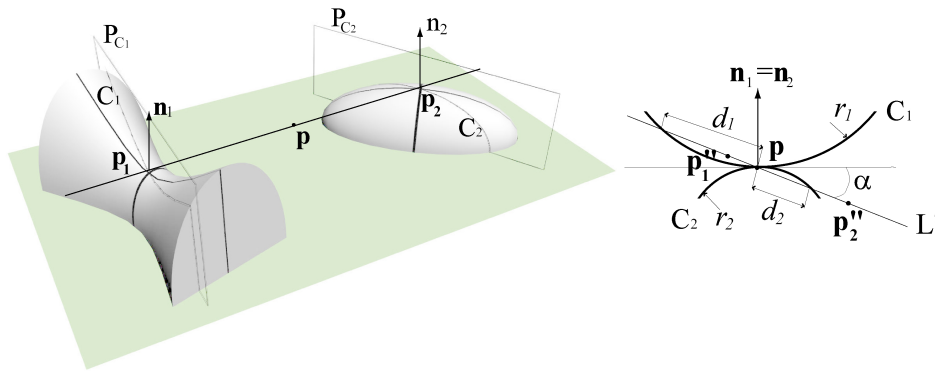where θ is the angle with the first principal direction.

Fig. 14

Let us consider the projection onto P of the various geometrical entities. The curvatures of the projections of C_1 and C_2, which can be approximated near the projections of $\mathbf{p}_1$ and $\mathbf{p}_2$ by two infinitesimal segments of the osculating circles, are easily found dividing the 3D curvatures by the cosines of the angles between P_{C1}, PC2 and the projection plane. Let r_1 and r_2 be the radiuses of curvature of these projections, (see Fig. 14). In order to obtain a visual line L', the projections of $\mathbf{p}_1$" and $\mathbf{p}_2$" must lie on the external sides of the projections of C_1 and C_2. Then the lengths in P of the two segments $\mathbf{p}_1$"$\mathbf{p}$ and $\mathbf{pp}_2$» must satisfy the following inequalities:

$| \mathbf{p}_1\text{"}\mathbf{p} |_P < d_1$

$| \mathbf{p}\ \mathbf{p}_2\text{"}|_P > d_2$

where d_1 and d_2 are the length of the segments in P intercepted by the projections of C1 and C_1 on the projection of L'. It follows that

$| \mathbf{p}_1"\mathbf{p} |_P / | \mathbf{p}\,\mathbf{p}_2"|_P < d_1 / d_2$ (*)

Let $|\mathbf{p}_1\mathbf{p}|$ and $|\mathbf{p}_2\mathbf{p}|$ be the finite 3D distances between $\mathbf{p}$ and the tangency points $\mathbf{p}_1$ and $\mathbf{p}_2$ (see Fig. 14). We have

$| \mathbf{p}_1"\mathbf{p} |_P / | \mathbf{p}\,\mathbf{p}_2"|_P = |\mathbf{p}_1\mathbf{p}| / |\mathbf{p}_2\mathbf{p}|$

In addition, for any angle α it is

$d_1 / d_2 = r_1 / r_2$

Then (*) becomes

$|\mathbf{p}_1\mathbf{p}| / |\mathbf{p}_2\mathbf{p}| < r_1 / r_2$ (**)

Concluding, only through points that satisfy (**) pass visual lines compatible with the local geometry. It follows that the internal segment of L' consists of an inactive segment $\mathbf{p}_1\mathbf{p}^*$ and a locally active segment near $\mathbf{p}^*\mathbf{p}_2$ such that

$|\mathbf{p}_1\mathbf{p}^*| / | \mathbf{p}^*\mathbf{p}_2| = r_1 / r_2$

3.2 Locally Active Segments of Bi-tangent Lines for $n_1 = -n_2$

Observe first that only the exterior half-open segments can be locally active. This is immediately seen by inspecting the section of $\mathbf{O}$ made by the plane P_N containing $\mathbf{n}_1$ and $\mathbf{n}_2$, as can be seen in Fig.4(d). Thus we must only investigate the two external half-open segments.

The possible cases are six as before. For brevity, will not report here a detailed analysis for the first five cases, since they are similar to the corresponding cases of the previous subsection.

The results are as follows. The cases *elliptic-elliptic* and *elliptic-parabolic* are not active. As before, it is not necessary to deal with the case *parabolic-parabolic*. Both the cases *parabolic-hyperbolic* and *hyperbolic-hyperbolic* produce locally active exterior segments.

As in the previous section, the case *hyperbolic-elliptic* requires a detailed analysis involving the curvatures of the contour generators. Let us consider first (Fig.15) the external segment starting at $\mathbf{p}_2,$ the elliptic point.
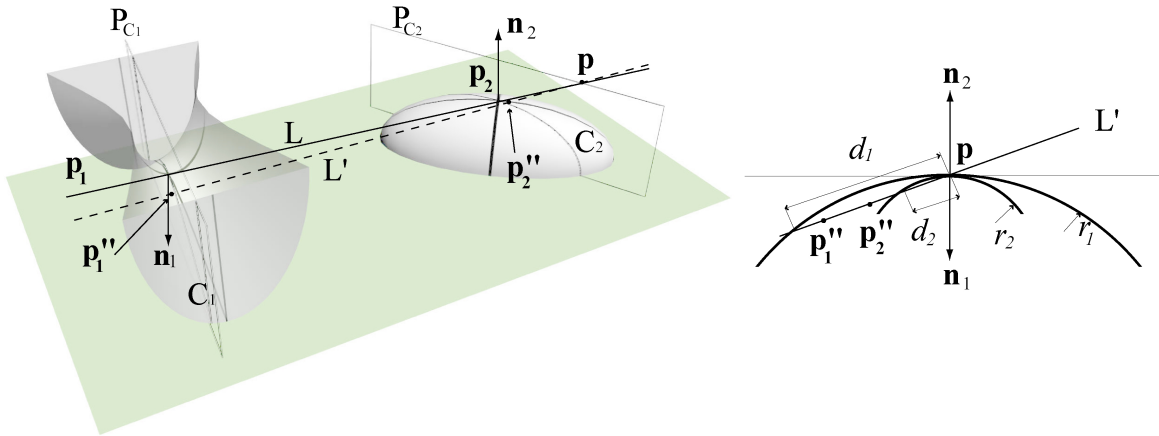
Fig. 15

As before, the condition for a line passing through a point $\mathbf{p}$ of this segment to be a visual line is (Fig. 15)

$$| \mathbf{p_1"p} |_P < d_1$$

$$| \mathbf{p\ p_2"} |_P > d_2$$

that is

$$|\mathbf{p_1p}| / |\mathbf{p_2p}| < r_1/r_2 \qquad\qquad (*)$$

Let us assume $r_1 > r_2$, as in Fig. 15, so that $1 < r_1/r_2$. Clearly, the inequality (*) is not verified for points near $\mathbf{p_2}$. The external segment is divided into one locally active part $\mathbf{p_2p^*}$ and an inactive part $\mathbf{p^*\infty}$. The point $\mathbf{p^*}$ is such that

$$|\mathbf{p_1p^*}| / |\mathbf{p_2p^*}| = r_1/r_2$$

If $r_1 \leq r_2$, that is $1 \geq r_1/r_2$, no $\mathbf{p}$ can satisfy (*) and the complete external segment is locally active.

Now let us consider the external segment starting at $\mathbf{p_1}$, the hyperbolic point (Fig.16).
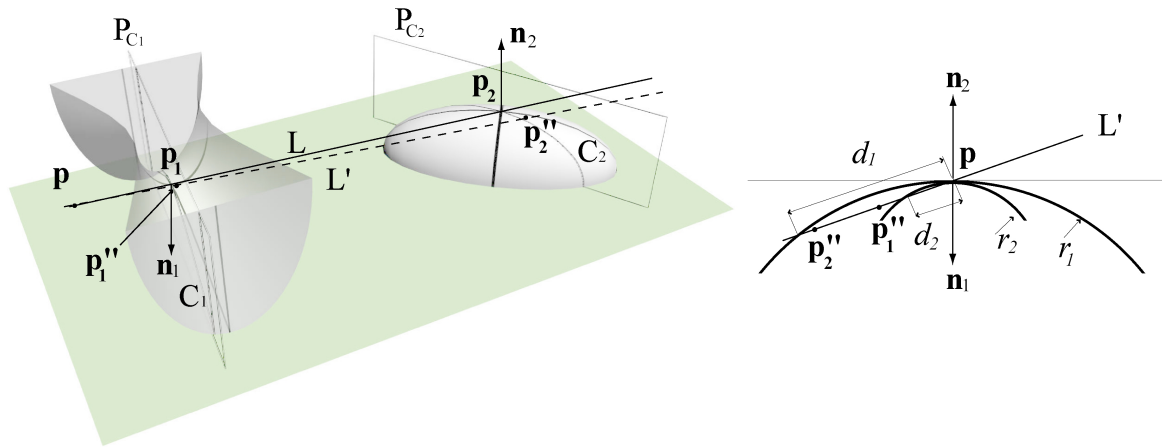
Fig. 16

As in the previous case, for a visual line to pass through a point $\mathbf{p}$ it must be $|\mathbf{p}_1\mathbf{p}| / |\mathbf{p}_2\mathbf{p}| < r_1 / r_2$ (Fig. 16). If $r_1 \geq r_2$, that is $r_1 / r_2 \geq 1$, as in Fig. 16, any $\mathbf{p}$ can satisfy the inequality and the external segment is inactive. If $r_1 < r_2$, that is $r_1 / r_2 < 1$, the inequality is satisfied only by points of a segment $\mathbf{p}_1\mathbf{p}^*$, which is inactive. The remaining segment $\mathbf{p}^*\infty$ is locally active. Again, the position of $\mathbf{p}^*$ is such that $|\mathbf{p}_1\mathbf{p}^*| / |\mathbf{p}_2\mathbf{p}^*| = r_1 / r_2$.

3.3. Locally Active Segments of Tri-tangent Lines

Let $\mathbf{p}_1$, $\mathbf{p}_2$ and $\mathbf{p}_3$ be the tangency points of L, and E_1, E_2 and E_3 the orthographic projections along L of infinitesimal segments of the contour generators containing $\mathbf{p}_1$, $\mathbf{p}_2$ and $\mathbf{p}_3$.
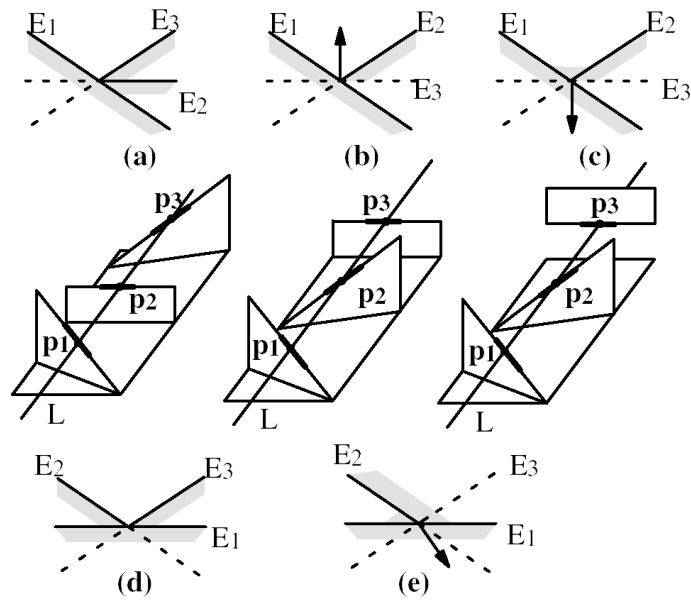
Fig.17. The possible arrangements of the limbs for tri-tangent lines

Three spatial arrangements of the limbs, shown in Fig.17. (a), (b) and (c), are possible. For each case the figure shows the orthographic projection along L and an assonometric view. In the orthographic projection the arrow, pointing outside the object, marks a limb covered by the others. In the assonometric views only the short segments (actually infinitesimal) marked with a thicker line belong to S. The origami-like structure is intended to clarify the relative 3D position of the contour generators.

Inspecting the orthographic projections could suggest that two other cases exist, shown in Fig.17 (d) and (e). Actually, cases (d) and (e) are cases (b) and (c) observed from the opposite side. Case (a) produces the same projections from both sides.

The tri-tangent line L is divided into two interior open segments and two half-open exterior segments. In order to determine the locally active segments, for each case we will consider the possible visual lines passing through points of L and lying in a plane P_R rotating about L. The trace of P_R in the orthographic projection plane can lie in three different areas, marked as 1, 2 and 3 for case (a) in Fig.18 (a).
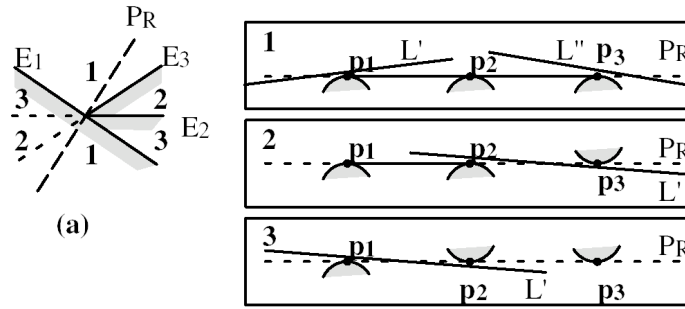
Fig.18. Arrangement (a) does not yield active segments

The figure also shows, for case (a), the three possible intersections of P_R and S. The first intersection shows that the exterior segments are inactive, since small rotations of L about any point of these segments produce visual lines as L' and L". Intersections 2 and 3 show that also the interior segments are inactive. Concluding, case (a) does not produce active segments.

We omit for brevity a similar analysis for cases (b) and (c). The results obtained are summarized in Fig.19, where the locally active segments of tri-tangent lines are solid.
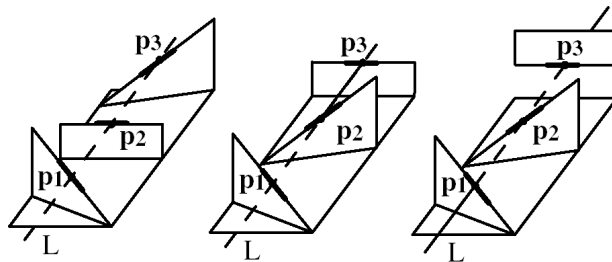

Fig.19. The locally active segments of tri-tangent lines.

4. AN ALGORITHM FOR COMPUTING THE VISUAL HULL

Constructing an algorithm for computing the visual hull of a smooth curved object can be done by modifying the algorithm implemented by Kriegman, Petitjean and Ponce [28] for computing the aspect graph of smooth curved objects. The techniques described in [28] for solving the systems (1) and (2), or the equivalent systems for implicit surfaces, can be used for obtaining the pairs p_1 and p_2 for the visual event tangent crossing, and the triplets p_1, p_2 and p_3 for the visual event triple point. The corresponding bi or tri-tangent lines passing through these points produces

the relevant boundary surfaces. For obtaining the locally active patches, we must discard the surfaces, or their parts, which:

1) do not satisfy the local necessary conditions determined in Section 3;

2) intersect S.

By intersecting all the locally active patches we construct a partition of R^3. Each cell of this partition belongs entirely or does not belong at all to the visual hull, and the whole visual hull can be constructed by checking each cell and merging with **O** those belonging to the visual hull. To check a cell, chose a random point in it, and construct the cone formed by the lines passing through the point and tangent to **O**. The cell belongs to the visual hull if all the tangent lines also intersect **O**.

The complexity of the visual hull algorithm is bounded by the complexity of the algorithm for computing the perspective aspect graph. For algebraic surfaces of degree g, it has been found [29] that this complexity is $O(g^{18})$, due to the tri-tangent surfaces.
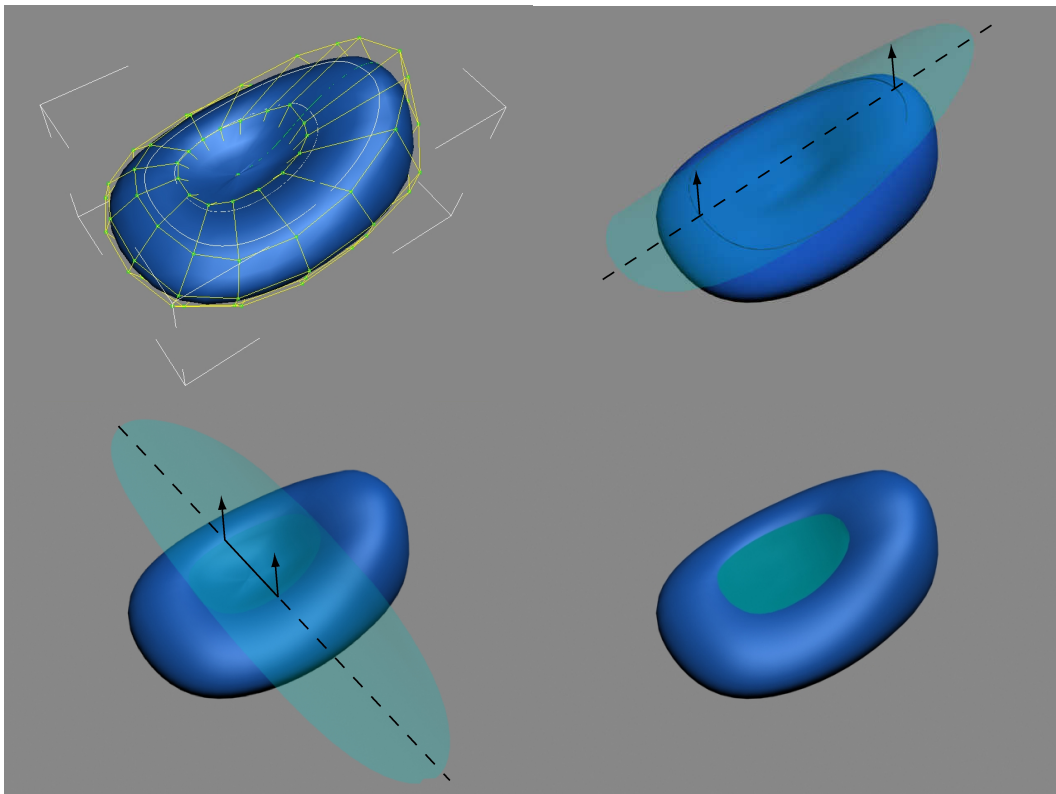

Fig. 20

An example is shown in Fig. 20. The object, with a simple concavity, has been modeled as a closed smooth NURBS surface. At the upper left of the figure we show the object shaded and the net of control points. The object generates two surfaces both related to the visual event tangent crossing. The surface shown on the upper right of the figure is inactive since the tangency points are all elliptic. The other surface formed by bi-tangent lines is shown at the lower left. This surface is locally active, since for all tangent lines the tangency points are hyperbolic. The visual hull, where the concavity is covered by the only locally active patch, is shown on the lower right.

5. CONCLUSIONS

In this paper we have developed the theory of the visual hull of smooth curved objects. A main result is the link established between the visual hull and the aspect graph of these objects. We have shown that $S''_{VH,}$ the surface of the visual hull not coincident with the surface S of the original object, consists of patches of the boundary surfaces of the viewing space of the aspect graph. These surfaces correspond to the visual events tangent crossing and triple point of smooth curved objects.

We have also shown that only in some cases patches of these surface can bound the visual hull, and we have determined these cases by inspecting the geometry of the surface S at the tangency points. We have also outlined an algorithm for computing the visual hull, which in part exploits an algorithm implemented for computing the aspect graph. Future work will be aimed at extending these results to more general curved objects.

APPENDIX

Let us consider the local approximation $2z = k_1(\mathbf{p}^*)x^2 + k_2(\mathbf{p}^*) y^2$ of the surface S near an elliptic point $\mathbf{p}^*$, a line L tangent to the surface at $\mathbf{p}^*$, and point $\mathbf{p'}$ lying on L. Let, in the local coordinate system, be $\mathbf{p'} = (X' \ Y' \ 0)$ (see Fig. 21).
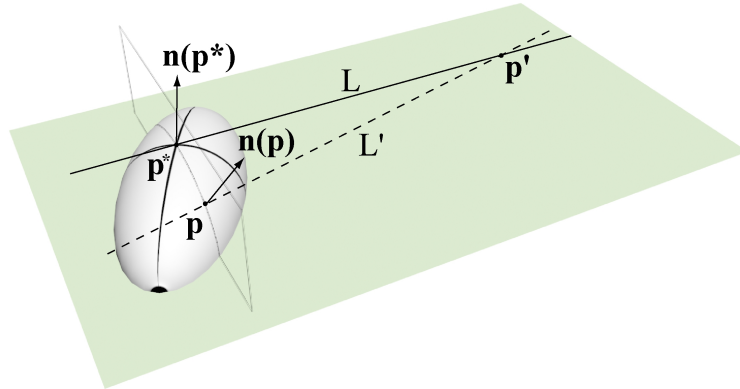
Fig. 21

A vector $\mathbf{n}(\mathbf{p})$ normal to the surface at a generic point $\mathbf{p}=(x \quad y \quad z)= (x \quad y \quad \tfrac{1}{2}(k_1(\mathbf{p}^*)x^2 + k_2(\mathbf{p}^*) y^2))$ is easily found as the vector product of the tangent vectors along the principal directions $\mathbf{t}_1$ and $\mathbf{t}_2$:

$\mathbf{n}= \mathbf{t}_1 \text{ x } \mathbf{t}_2= (\,0 \quad 1 \quad k_1(\mathbf{p}^*)x)\text{x}(1 \quad 0 \quad k_2(\mathbf{p}^*)\,y)) = (\text{-} k_1(\mathbf{p}^*)x \quad \text{-} k_2(\mathbf{p}^*)\,y \qquad 1)$

Let us rotate L about $\mathbf{p'}$ of an infinitesimal angle in such a way that the rotated line is tangent to S at a point $\mathbf{p}$. The rotated line $\mathbf{pp'}$ must be normal to $\mathbf{n}(\mathbf{p})$. Hence their dot product must be 0:

$\mathbf{n}(\mathbf{p})\bullet \mathbf{pp'}=(\text{-} k_1(\mathbf{p}^*)x \quad \text{-} k_2(\mathbf{p}^*)\,y \qquad 1) \bullet (X'\text{-}x \qquad Y'\text{-}y \quad \text{-} \tfrac{1}{2}(k_1(\mathbf{p}^*)x^2 + k_2(\mathbf{p}^*)\,y^2)) =0$

and then

$k_1(\mathbf{p}^*)X'x +(k_1(\mathbf{p}^*)x^2\text{-} k_2(\mathbf{p}^*)Y'\,y + k_2(\mathbf{p}^*)\,y^2\text{-} \tfrac{1}{2}(k_1(\mathbf{p}^*)x^2 + k_2(\mathbf{p}^*)\,y^2)=0$

Neglecting second order terms, we obtain

$x/y = \text{-} (k_2(\mathbf{p}^*)/k_1(\mathbf{p}^*))Y'/X'$

This means that the curve formed by tangency points $\mathbf{p}$ can be obtained by intersecting the surface S with a plane passing through the axis Z and forming with the principal directions Y an angle whose tangent is given by the above formula. Observe that neglecting second order terms means assuming that the line, rotated by an infinitesimal angle about a point $\mathbf{p'}$ lying at a finite distance from $\mathbf{p}$, is parallel to L. Then the curve formed by the tangency point is arbitrarily near, approaching $\mathbf{p}^*$, to the contour generator for viewlines parallel to L.

The above results also hold for an hyperbolic point. The only difference is that, since the principal curvatures have opposite signs, in the plane XY the line L and the trace of the plane containing the contact curve are in the same quadrant.

6. REFERENCES

[1] N. Ahuja and J. Veenstra: Generating octrees from object silhouettes in orthographic views, *IEEE Trans. on PAMI*,Vol.11,pp.137-149,1989

[2] V.I.Arnold, *Catastrophe Theory,* Springer-Verlag, Heidelberg,1984

[3] K.W. Bowyer and C.R. Dyer, "Aspect Graphs: An Introduction and Survey of Recent Results," *Int'l J. Imaging Systems and Technology,* vol.2, pp. 315-328, 1990

[4] K.Bowyer , M. Sallam, D.Eggert and J. Stewman, "Computing the Generalized Aspect Graph for Objects with Moving Parts," *IEEE Trans. Pattern Analysis and Machine Intelligence,* vol.15, no.6, pp.605-610, 1993

[5] J.Callahan and R. Weiss, "A Model for Describing Surface Shape," in *Proc. IEEE Conf. on Comp. Vision and Pattern Recognition,* pp. 240-245, 1985

[6] C. H. Chian and J. K. Aggarwal: Model reconstruction and shape recognition from occluding contours", *IEEE Trans.on PAMI*, Vol.11, pp.372-389, 1989

[7] M. Demazure, "Catastrophes et bifurcations,"Edition Ellipses, 1989

[8] F. Durand, G. Drettakis and C. Puech, "The 3D visibility complex: a unified data-structure for global visibility of scenes of polygons and smooth objects," *Proc. 9th Canadian Conference on Comput. Geometry,* Kingston, Canada, pp. 153-158, 1997

[9] F. Durand, G. Drettakis and C. Puech, "The 3D visibility complex ,"*ACM Trans. On Graphics,* Vol. 21. no.2, pp.176-206, 2002

[10] D.W. Eggert , K.W. Bowyer, C.R. Dyer, H.I. Christensen, and D.B. Goldof, "The Scale Space Aspect Graph, "*IEEE Trans. Pattern Analysis and Machine Intelligence,* vol.15, no.11, pp.1,114-1139, 1993

[11] D.Eggert and K.Bowyer," Computing the Perspective Aspect Graph of Solids of Revolution,"*IEEE Trans. Pattern Analysis and Machine Intelligence,* vol.15, no.2, pp.109-128, 1993

[12] D. A. Forsyth, "Recognizing algebraic surfaces from their outlines," *Int. J. of Computer Vision*, vol. 18, no.1, pp.21-40, 1996

[13] J.J. Gibson, "What is a form?" *Psychol. Rev.,* vol.58, pp. 403-412, 1951

[14] Z.Gigus, J.Canny, and R. Seidel, "Efficiently computing and representing aspect graphs of polyhedral objects," ," *IEEE Trans. Pattern Analysis and Machine Intelligence,* vol.13, no.6, pp. 542-551, 1991

[15] Y.K. Kergosien,"La Famille des Projections Orthogonales d'Une Surface et Ses Singularités," *C.R. Acad.Sc.Paris,* 292, pp.929-932, 1981

[16] J. J.Koenderink and A. J. van Doorn," The Singularities of the Visual Mapping," *Biol. Cybern.* vol.24, pp.51-59, 1976

[17] J. J.Koenderink and A. J. van Doorn," The Internal Representation of Solid Shapes with Respect to Vision," *Biol. Cybern.* vol.32, pp.211-216, 1979

[18] D.J. Kriegman and J.Ponce, "On recognizing and positioning curved 3D objects from image contours," *IEEE Trans. Pattern Analysis and Machine Intelligence,* vol.12, no.12, pp.1127-1137, 1990

[19] A. Laurentini," The Visual Hull Concept for Silhouette-based Image Understanding*," IEEE Trans. Pattern Analysis and Machine Intelligence,*vol.16, pp.150-162, 199

[20] A. Laurentini, "Computing the Visual Hull of Solids of Revolution," *Pattern Recognition,* vol. 32, pp.377-388, 1999

[21] A. Laurentini ," How Far 3-D Shapes Can Be Understood from 2-D Silhouettes," *IEEE Trans. Pattern Analysis and Machine Intelligence*, vol. 17, pp.188-195, 1995

[22] A. Laurentini, "Surface Reconstruction Accuracy for Active Volume Intersection," *Pattern Recognition Letters,* vol. 17, pp. 1285-1292, 1996

[23] A. Laurentini," How Many 2D Silhouettes it Takes to Reconstruct a 3D Object," *Comput. Vision and Image Understanding*, vol.67, pp. 81-87, 1997

[24] P. Mendonca, K.Wong and R. Cipolla, "Epipolar geometry from profiles under circular motion," *IEEE Trans. Pattern Analysis and Machine Intelligence*, vol. 23, pp.604-616, 2001

[25] B.O'Neill, *Elementary Differential Geometry*, Academic Press, San Diego, 1996

[26] O.A. Platonova, "Singularities of projections of smooth surfaces," *Russian Math. Surveys,* . 39, pp.177-178, 1984

[27] S. Petitjean,"A Computational Geometric Approach to Visual Hull," *Int. J. of Comput. Geometry and Appl.*, vol. 8, no.4, pp. 407-436, 1998

[28] S.Petitjean, J.Ponce and D.J.Kriegman, "Computing exact aspect graphs of curved objects: algebraic surfaces," *Int. J. of Computer Vision*, vol. 9, no.3, pp.231-255, 1992

[29] S.Petitjean," The enumerative geometry of projective algebraic surfaces and the complexity of aspect graphs," *Int. J. of Computer Vision*, vol. 19, pp.1-29, 1996

[30]M. Pocchiola and G. Vegter, "The Visibility Complex," *Int. J. of Comput. Geometry and Appl.*, vol. 6, no.3, pp. 279-308, 1996

[31] J. Rieger, "On the classification of views of piecewise smooth objects," *Image Vis. Comput.* Vol.5, pp. 91-97, 1987

[32] J. Rieger, "The geometry of view space of opaque objects bounded by smooth surfaces," *Artificial Intelligence,* Vol. 44, pp. 1-40, 1990

[33] I. Shimshoni and J.Ponce, "Finite Resolution Aspect Graphs of Polyhedral Objects," *IEEE Trans. Pattern Analysis and Machine Intelligence,* vol.19, no.4, pp.315-327, 1997

[34] T. Sripradisvarakul and R. Jain," Generating aspect graphs for curved objects," *Proc. IEEE. Workshop on Interpretation of 3D Scenes,* pp. 109-115,1989

[35] J. Y. Zheng: Acquiring 3D models from sequences of contours, *IEEE Trans. on PAMI*, Vol. 16, no.2, pp.163-178,1994